

# A Corrosion Model for prediction of Service Life of Reinforced Concrete water structures.

Philip Mogire<sup>1,a,\*</sup>, John Mwero<sup>2,b</sup>, Silvester Abwodha<sup>3,c</sup> and Geoffrey Mang'uriu<sup>4,d</sup>

<sup>1,2,3</sup>Department of Civil and Construction Engineering,  
University of Nairobi, Kenya

<sup>4</sup>Department of Civil, Construction and Environmental Engineering,  
Jomo Kenyatta University of Agriculture & Technology  
P.O. Box 62000-00200, Nairobi, KENYA

<sup>a</sup>philosiemo@yahoo.com, <sup>b</sup>johnmwero1@gmail.com, <sup>c</sup>sochieng@yahoo.com, <sup>d</sup>gmanguriu@yahoo.co.uk  
\*corresponding author

DOI: 10.29322/IJSRP.10.02.2020.p98104  
<http://dx.doi.org/10.29322/IJSRP.10.02.2020.p98104>

**Abstract-** As the world economies endeavor to support the United Nations sustainable development goals, new technologies are evolving for efficient design and manufacture of civil engineering products. Researchers have up scaled their effort to develop techniques to monitor the performance of civil engineering structures within their service life for optimum return from investment. The aim of this research was to develop a service life model to for prediction of the service life of reinforced concrete water conveyancing structures.

To achieve the desired objective, steel samples were cast in concrete of characteristic strength of 25N/mm<sup>2</sup>, 9 cylinders each of 150mm diameter x 300mm long, 130mm diameter x 300mm long and 100mm diameter x 300mm long respectively in concrete characteristic strength 25N/mm<sup>2</sup>, 30N/mm<sup>2</sup> and 35N/mm<sup>2</sup> for accelerated corrosion test were cast. After 24 hours the cast specimens were demolded and immersed in curing tanks for 27 days and then immersed in a 3.5% industrial sodium chloride solution under 6V. The accelerated corrosion specimens were monitored for onset of cracks and stopped when the cracks were 0.2mm in width.

The physical and chemical properties of the materials were investigated for compliance to relevant applicable British and Kenyan standards for conformity to acceptable criteria. The concrete materials were batched by weight and mixed by a lab electric pan concrete mixer in batches of 0.009 m<sup>3</sup>. The concrete batches were tested for consistency by the slump and compaction factor tests.

From the results a model that takes account of the cover to the rebar, the rebar size and the compressive strength properties of concrete and steel/concrete interface was developed.

The model developed here is for water structures and shows that the time to corrosion cracking of the cover concrete in a chloride contaminated concrete structure is a function of reinforcement cover, corrosion rate and critical mass of the corrosion products. The times to cracking predicted by the model are in good agreement with the observed times to cracking based on this research

**Index Terms-** Accelerated corrosion, water structures, Corrosion model.

## 1. INTRODUCTION

Building on the millennium development goals, in a transformative, inclusive, comprehensive and integrated agenda 2030, the 17 Sustainable Development Goals (SDGs) for Sustainable Development were adopted in September 2015 by 193 countries [1]. The SDGs address humanitarian and environmental problems including poverty, education, health, biodiversity, and climate change (United Nations, 2016). Attention has turned to designing and implementing policies to achieve The SDGs by the designated completion year of 2030. Kenya, among many governments in the developing world have encouraged developing of small hydropower projects to increase power capacity which in turn will accelerate achievement of the 17 SDGs. Each of the small hydropower projects has a reinforced concrete conveyance or diversion structure that require assessment of their performance within their service life. Research in the deterioration models for reinforced concrete water structures is key in their sustainable performance.

Deterioration of reinforced concrete due to corrosion which results from carbonation or from chloride ingress plays a significant role in reduction of the design service life of reinforced concrete water structures and has attracted researchers of various disciplines during the past three decades [2]. Metals store heat as potential energy during their production and release this energy during the corrosion process after reacting with the favorable corrosive environment. These will tend to lose their energy by reverting to compounds more or less similar to their original states, for example the starting material for iron and steel making and the corrosion product rust has the same chemical composition (Fe<sub>2</sub>O<sub>3</sub>). The energy stored during melting and released during corrosion supplies the driving potential for the corrosion process to take place [3], therefore corrosion occurs when at least two metals (or two locations of the reinforcing bar) is at different energy levels. In reinforced concrete the concrete acts as an electrolyte while the rebar act as a metallic connection [4]. At a

pH of 12- 13, reinforced concrete is in an alkaline state and a thin oxide layer forms on the steel and prevents metal atoms from dissolving forming a passive film [5]. The passive film reduces the corrosion rate to an insignificant level without which the steel would corrode at rates at least 1,000 times higher [6].

The presence of rust on reinforcement bars and appearance of cracks parallel to the reinforcement bars is an indication of the presence of corrosion in reinforced concrete structures. Carbonation inducing a generalized attack and the presence of chlorides inducing a localized attack are the main causes of electrochemical corrosion in reinforced concrete as shown in Figure 1[4]. Carbonation induced corrosion commonly occurs in relatively dry environments where sufficient carbon oxide to diffuse into the cover concrete is possible. In chloride containing environments, the chloride ingress is usually faster than the carbonation process, and it is more likely to be the predominant cause of deterioration in reinforced concrete water structures by degrading the resistance of the structure to service loads.

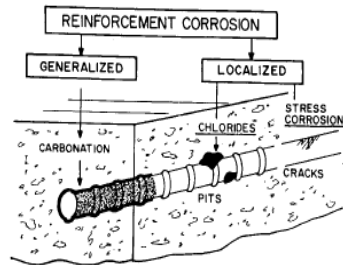


**Figure 1: Types and morphology of the corrosion in concrete: generalized (carbonation), localized (chlorides) [4]**

When reinforcement corrosion becomes visibly detected, deterioration has already occurred and it may be too late to take any corrective or protection measures. This makes the reinforced concrete service life prediction models very critical for any sustainable structure. The permeability of the concrete, nature and force of cracks, and the cover thickness have an incredible role on the start and progression of corrosion.

Various corrosion models have been proposed and can broadly be categorized into either empirical [7], analytical [8-10] or numerical [11-12]. Molina et al. [11] used a smeared crack model for the finite element analysis of cover cracking due to reinforcement corrosion. In their model they presumed corrosion of steel to take a linear variation of the material properties from those of steel to those of rust. Due to lack of information they also assumed that the mechanical properties of rust nearly resemble that of water which is one of the main constituents of rust. Their analysis was based on the experiments of Andrade et al. [13] where the thickness of the concrete cover was 1.25 and 1.9 times the reinforcement diameter.

An empirical equation for predicting the time to cover cracking without reference to the evolution of the damage zone was suggested by Morinaga [14]. In his empirical equation; the time to cover cracking as a function of the corrosion rate, concrete cover thickness and reinforcing diameter was accounted. In close scrutiny of Monariga's results shows that the cover cracking predicted by Morinaga's model is much shorter than the experimentally observed values[15], [16].

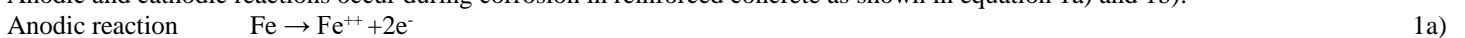
Further investigations in this field have revealed that the consideration of the appropriate mechanical behavior of corrosion products strongly affects the predicted results [17]. Lundgren [18], in an effort to study rebar pull-out, presented a reasonable way to model the effect of corrosion on the bond between the corroded reinforcement and concrete. Lundgren employed finite element analysis and assumed that rust behaves like granular materials, in accordance with the experimental tests of Andrade et al. [19]. Lundgren pointed out that the model could predict the decrease of the bond when splitting of the concrete occurs. It was emphasized that axisymmetric analysis appears to be a satisfactory level of modeling when a study of concrete cover cracking due to uniform corrosion is of concern. However, three dimensional models should be used if localized corrosion is to be studied.

Bhargava et al. [20],[21] presented a mathematical model to predict the time to concrete cover cracking and weight loss of reinforcing bars. However, they assumed that the mechanical properties of corrosion products are the same as those of steel, though reasonably good agreement was obtained between experimental results and the analytical predictions. They showed that tensile strength, initial tangent modulus of concrete, annual mean corrosion rate, and modulus of elasticity of the reinforcement and corrosion significantly influence the predicted time to cover cracking.

In this study a mathematical model is formulated to determine the corrosion rate in water conveyancing structures. This model takes into consideration of the serviceability limiting condition of the crack width of water structures.

## **2. CORROSION INDUCED REINFORCED CONCRETE CRACKING MODEL FOR A WATER CONVEYANCING STRUCTURE**

Anodic and cathodic reactions occur during corrosion in reinforced concrete as shown in equation 1a) and 1b):



Initially, the rate of corrosion will depend on the chloride concentration and the rate of the anodic reaction. Shortly thereafter, as the corrosion becomes more severe and the rust layers build up, the corrosion rate will be controlled by the cathodic reaction and the availability of oxygen at the cathode. The structure of the pit and corrosion products depends on the aqueous phase of the pore solution, rebar type, and pressure adjacent to the bar. Generally, the composition of the expansive corrosion products may be expressed as shown in equation 2:

Corrosion product  $\rightarrow \{a.Fe(OH)_2 + b.Fe(OH)_3 + c.H_2O\}$  [22] 2)  
 where  $a, b$  and  $c$  are variables that depend on the alkalinity of the pore water solution of the concrete, the oxygen supply, and the moisture content.

During progression of corrosion of reinforcement bars in reinforced concrete, the oxidation products increase in volume. The corrosion products take up more volume than the virgin steel rebar and therefore, are inclined to deteriorate the concrete by producing tensile stresses as well as microcracks nearby the rebar. The expansion ratio of the oxide to the original rebar volume depends on the specific type of oxide formed [23]. Depending on the oxidation level, the volume increase due to rebar corrosion is around 2.0 to 6.5 times the original rebar volume [22]. The production of rust may follow a linear or parabolic law depending on the rust properties [24]. When corrosion of reinforcement develops significantly, the corrosive products expand continuously and generate internal pressure to the concrete surface around the steel bar. The continuous process of reinforcement corrosion affects structural serviceability by cracking, spalling the concrete cover and also decreasing the load-bearing capacity thus endangering the structural safety. The physical effects of corrosion include loss of steel area, loss of bond strength between steel reinforcing bars and concrete and reduction of concrete composite strength due to cracking. In this research, a service life model is developed utilizing the results of accelerated corrosion.

A considerable research has been undertaken on corrosion of reinforced concrete. On experimental work on corrosion induced cracking in reinforced concrete, the corrosion process is usually accelerated by various means so that concrete cracking can be achieved in a relatively short time [15]. Due to carbonation or in the presence of chlorides, corrosion is initiated by the breakdown of a 'passive layer'. The composition, pore structure and cover of concrete play a big role in corrosion initiation period as well as rate of corrosion. The rate of corrosion is often modeled using Faraday's law. The pH driven corrosion reaction rate is current density dependent. The resulting mass loss to oxidation for a constant current time interval according to Faraday's law is:

$$\Delta W = (ITA) / (ZF) \quad [25] \quad 3)$$

Where  $\Delta W$  = weight loss (grams)

$I$  = corrosion current (amp)

$T$  = time (sec)

$A$  = atomic weight of iron (56g)

$Z$  = valency of the metal (2)

$F$  = Faraday constant (96500 Amp-sec).

By inserting the specific values of  $A, Z,$  and  $F$  into eq. (3), the rebar mass conversion as a function of time and corrosion current is:

$$\Delta W = 25It \quad 4)$$

Where,  $I$  = corrosion current (amp)

$t$  = time (days).

$$\text{Corrosion Rate (mm/yr)} = 87.6 \times [w / (D \times A \times T)] \quad [26] \quad 5)$$

where  $W$  is the weight loss in milligrams,

$D$  is the density of the corroding reinforcement in  $g/cm^3$

$A$  is the surface area of the specimen subjected to corrosion in  $(cm^2)$ , and

$T$  is the duration of the test period in hours.

### 3.0 Methodology

This study was conducted at the University of Nairobi Concrete and Materials lab where the physical properties of the materials, sample preparation and testing were done. The chemical properties of the ordinary Portland cement and chloride content was done at the State Department of Infrastructure in the Ministry of Transport, Infrastructure, Housing and Urban Development of the Government of Kenya.

#### 3.1 Concrete samples

The constituent materials for preparing test samples consisted of Ordinary Portland cement ( $42.5N/mm^2$ ), clean river sand, 20mm maximum size coarse aggregate and potable water.

##### 3.1.1 Cement

The chemical composition of the cement used in this research was tested. Available cements in Kenya are manufactured in accordance to KS EAS 18-1: 2001, an adoption of the European Norm EN 197 cement standards [27]. The cements locally available are produced for specific uses [28]. The Cement used for this research was ordinary Portland cement type 42.5N sourced from one wholesaler.

##### 3.1.2. Other concrete constituents

Table 1 shows the description and source of other constituents of concrete used in the research.

**Table 1. Details of materials used in the research**

SN	Description	Source	Remark
1.	Fine aggregates	Stockpile vender sourced from Machakos River	This was washed and oven dried before use.
2	Coarse aggregates	Kenya builders quarry	5-20mm uniformly graded at source
3.	10mm ribbed bars	Local manufacturer	Factory cut to 400mm
4.	Mixing water	Potable water in the Lab	

#### 3.2.2. Concrete Mix Design

With a characteristic strength of  $25\text{N/mm}^2$ , the concrete used was designed in accordance with the British Department of environment (DoE) method [29-30].

### 3.2.3 Test on hardened concrete

#### Compressive strength and split tensile strength

The compressive strength of concrete was investigated at 7, 14 and 28 days using a digital Universal Testing Machine shown in figure 2a), with a loading capacity of 2000 KN in accordance to BS EN 12390-3:2009 while the split tensile strength was done using a hydraulic Universal Testing machine as shown in figure 1b) and c).



Figure 2:a) Compression testing machine used in the research, b) and c) Failure mode during split tensile test

### 3.2.4 Accelerated Corrosion

#### 3.2.4.1 Materials and Specimens

This was done through an impressed corrosion test using the procedure below;

- i) 10mm diameter x 400mm long ribbed bars were polished with abrasive papers.
- ii) 120 mm of the surface length of each bar were sprayed with a zinc rich coating and left to naturally dry.
- iii) The mixed concrete (in two batches) was poured into 9 cylindrical samples of 150mm diameter and 300mm long, 130mm diameter and 300mm long, 100mm diameter and 300mm long each with a 10mm diameter rebar
- iv) The specimens were mechanically vibrated for 60s. After 24 hours, the cylindrical concrete specimens were demolded and cured for 27 days.
- vi) The test specimens were dried for 24 hours and then subjected to accelerated corrosion by storing them in a tank containing 3.5 % NaCl at room temperature and an impressed voltage of 6volts applied through a DC power supply regulator. The top and bottom surfaces of the concrete specimens were also sealed with Zinc rich coating so as to allow chloride ingress from the sides to simulate the corrosion of a section of a typical structural member in a water conveyancing structure.

#### 3.2.4.2 Testing Methodology

The accelerated corrosion set up is shown in Figure 3. The rebars projecting were connected in series to the anode and the stainless steel rod was connected to the negative terminal (cathode). The test specimens were subjected to a constant voltage of 6 V applied to the system using a DC power supply regulator. The variation in development of corrosion current was monitored at regular intervals using a high impedance multimeter and the average for the corrosion period taken for calculation of the average mass loss.

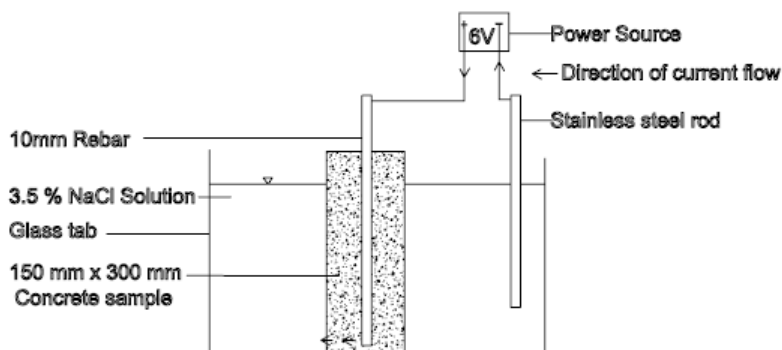
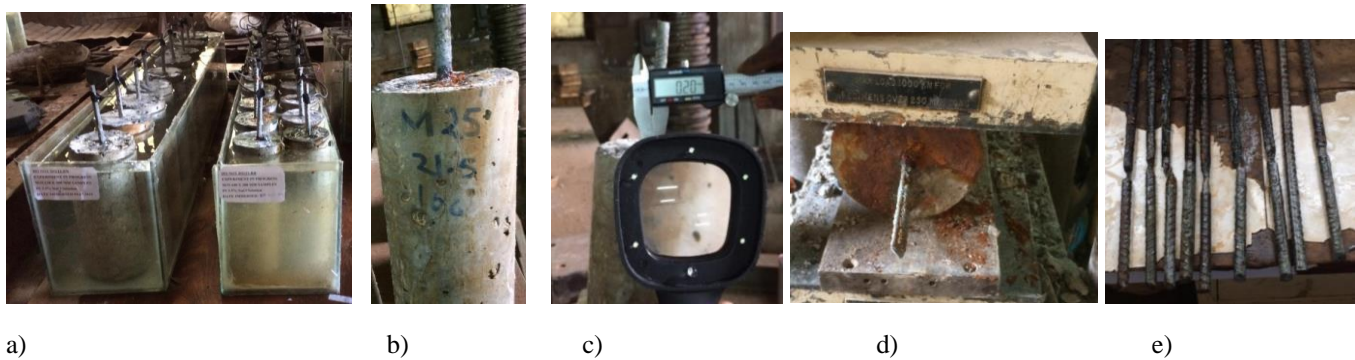


Figure 3:a) Schematic drawing of accelerated corrosion set up, b) Photo of the samples during experimentation

The appearances of first visible cracking were detected by visual observation using a magnification glass with power of x1000. The data collected for crack propagation provided the timing of first cracking and the subsequent time-dependent increase in crack width. After testing, the weight loss of bars due to corrosion were studied by cleaning, drying and weighing the reinforcement bars according to the

gravimetric weight loss method as specified by Standard Practice for Preparing, Cleaning, and Evaluating Corrosion Test Specimens (ASTM G1 – 90). Figure 4 shows samples during experimentation and measurement. The weight loss corresponded closely to that expected from current density ( $i_{corr}$ ) measurements.



**Figure 4: a) Samples during experimentation b) sample with 0.2mm longitudinal crack c) crack measurement d) recovering the corroded steel and e) cleaned rebar's for gravimetric weight loss measurement.**

### 3.3 Results of the material properties

#### i) Properties of aggregates

Various tests were carried out on the aggregates to determine their suitability for the research. Water soluble chlorides ions percent were found to be zero in fine aggregates, 0.002 % in coarse aggregates all less than 0.03% acceptable in compliance with BS EN 12620:2002.

**Table 2:Physical properties of aggregates used in the study**

Material	Specific gravity	Absorption %	Silt content %	Max Size
Fine aggregates	2.6	1.8	7.4	4.0
Coarse aggregates	2.6	0.3	0	20.0

**Table 3: Mechanical properties carried on coarse aggregates.**

Test	Size of aggregates mm	Crushing value %	Impact Value %	Flakiness index %	Loss Angeles Abrasion Value %
Result	5-20	18	8	35	20

#### ii) Chemical Properties of Cement used in the research

Table 4 shows results of the chemical composition of the cement used in the research. All the constituents of cement oxides were within the acceptable limits.

**Table 4 Result of Chemical composition the Cement used.**

SN	Test	Result of the sample	KS EAS 18-1: 2001 Requirement
1.	CaO%	59.11	Sum $\geq$ 50
2.	SiO <sub>2</sub> %	21.56	
3.	SO <sub>3</sub> %	2.78	$\leq$ 3.5
4.	MgO%	1.04	$\leq$ 5
5.	K <sub>2</sub> O%	0.051	
6.	Fe <sub>2</sub> O <sub>3</sub> %	3.48	
7.	Al <sub>2</sub> O <sub>3</sub>	8.09	3-8
8.	Na <sub>2</sub> O <sub>3</sub> %	0.018	
9.	LOI%	0.10	$\leq$ 5
10.	Cl%	0.016	$\leq$ 0.1
11.	IR%	0.55	$\leq$ 5

#### a)Effect of sum of lime (CaO) and silicon dioxide (SiO<sub>2</sub>) corrosion

The sum of lime (CaO) and silicon dioxide (SiO<sub>2</sub>) in the chemical analysis of ordinary Portland cement sample was 80.67%  $\geq$  50% within the acceptable limit [31]. This is consistent with the known fact that both CaO and SiO<sub>2</sub> give strength to concrete though SiO<sub>2</sub> has to be limited relative to CaO in order not to negatively affect setting time. The rate of corrosion is related to the strength of a concrete

sample while reduced setting time minimizes plastic shrinkage cracking and hence the rate of corrosion.

### b) Effect of CaO/SiO<sub>2</sub> on corrosion

The ratio of lime (CaO) to silicon dioxide (SiO<sub>2</sub>) contents in ordinary Portland cement should be greater than 2. The restriction on the ratio of lime to silicon dioxide [29] is to ensure that the quantity of silicon dioxide is considerably lower than that of lime so that the setting of concrete is not inhibited minimizing plastic shrinkage cracking.

### c) Effect of MgO on corrosion

The quantity of magnesium oxide (MgO) in ordinary Portland cement should not exceed 5% [32]. If the quantity of MgO is in excess of 5 percent, cracks will appear in concrete and which may affect the rate of corrosion by generating spots for penetration of chloride ions in concrete.

### d) Effect of SO<sub>3</sub> on corrosion

The quantity of sulphur trioxide (SO<sub>3</sub>) content in ordinary Portland cement was less than 3.5 % as required. SO<sub>3</sub> reduces the rate of transpassive layer dissolution inhibiting the onset of corrosion.

### e) Effect of Chloride Content on corrosion

The chloride content in ordinary Portland cement was less than 0.4% as required. Chloride ions in aqueous solution destroys the passivation film of rebars in the process of competing with hydrogen and oxygen ions in the adsorption process, thus leading to the occurrence of pitting corrosion, hole corrosion and crevice corrosion.

### f) Effect of Al<sub>2</sub>O<sub>3</sub> on corrosion

Aluminium oxide (Al<sub>2</sub>O<sub>3</sub>) reacts with free lime in concrete to form CaAl<sub>2</sub>Si<sub>3</sub>O<sub>12</sub>. which reduces the permeability of chloride and improving the corrosion resistance property of embedded steel in concrete. Above 8% the Al<sub>2</sub>O<sub>3</sub> will be in an active condition reducing the corrosion resistance.

### g) Effect of Fe<sub>2</sub>O<sub>3</sub> on corrosion

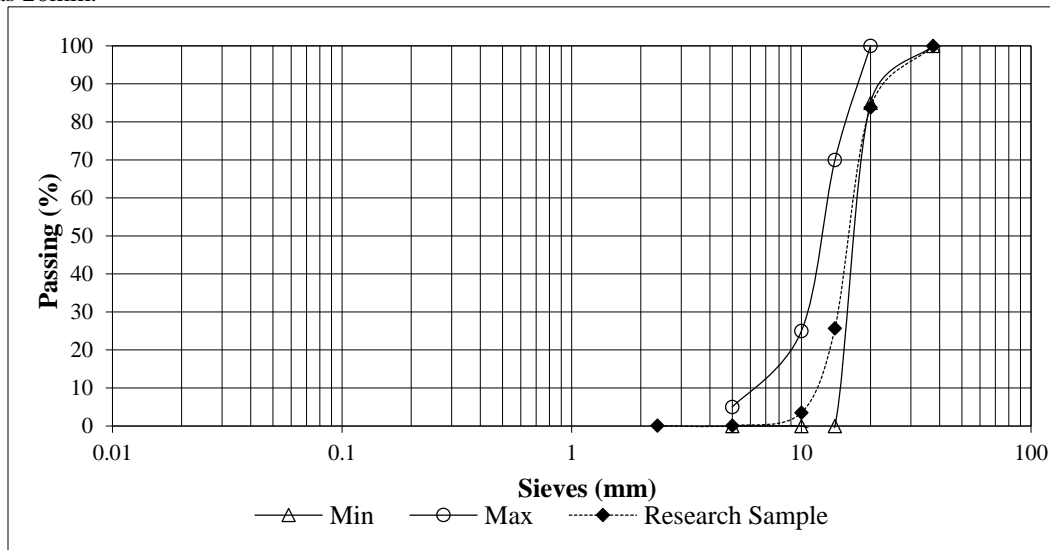
Iron oxide (Fe<sub>2</sub>O<sub>3</sub>) contributes to cement colour and helps in the fusion of the different ingredients. Fe<sub>2</sub>O<sub>3</sub> forms the passivation film reducing the oxygen diffusion rate, which, in turn, reduces the **corrosion** rate.

### h) Effect of Residues on corrosion

British standards consider Na<sub>2</sub>O, K<sub>2</sub>O, TiO<sub>2</sub> and P<sub>2</sub>O<sub>5</sub> in ordinary Portland cement as residues and limit the sum of all of them to 5%. If in excess of 5% efflorescence and unsightly cracking will occur aggravating corrosion.

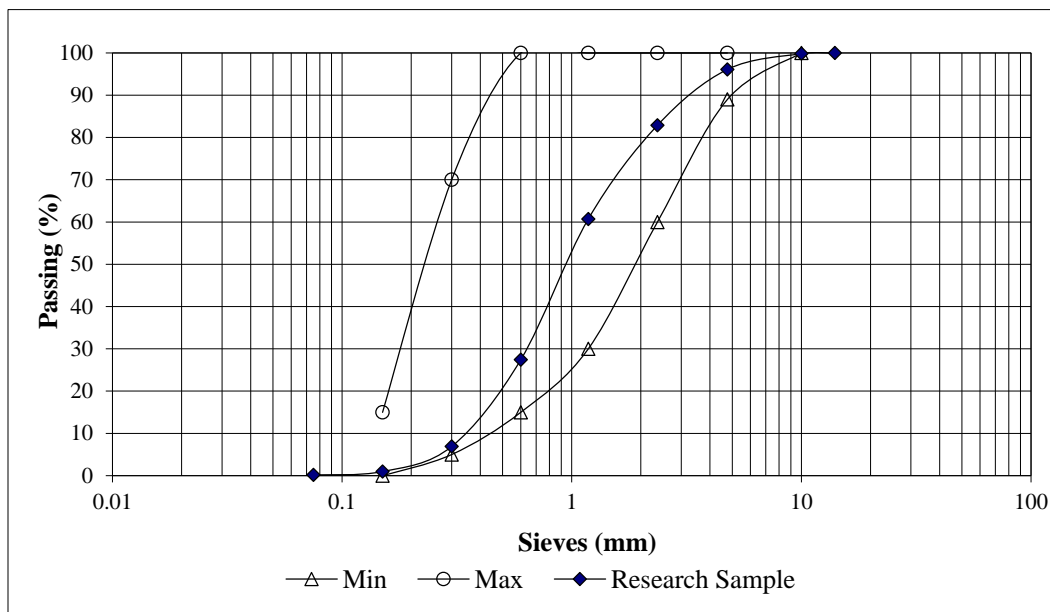
### iii) Gradation of Coarse and Fine aggregates

Particle size distribution analysis on a representative sample as shown on graph 1 of the coarse aggregates for the work was carried out to obtain the proportions by weight of the different sizes of coarse aggregates present. The sample is well graded with a maximum aggregate size was 20mm.



**Graph 1 Gradation of Coarse aggregates**

Particle size distribution analysis as shown on graph 1 on a representative sample of the fine aggregates for the research was carried out to obtain the proportions by weight of the different sizes of fine particles present according to BS 812-103 and BS 882. The proportions were expressed as percentages by weight passing various sieve sizes conforming to BS 410. As shown in graph 1 the coarse aggregates were well graded and expected to give a well interlocked composite concrete mix.



**Graph 2: Gradation of fine aggregates**

**iv) Results of hardened concrete**

**Table 4: Comparative study of results of hardened concrete for Concrete of characteristic strength 25 N/mm<sup>2</sup>**

Compressive strength (N/mm <sup>2</sup> ) at 28 days	Split tensile strength in N/mm <sup>2</sup>					
	Measured Value	Lavanya & Jegan (2015) $f_{t1}=0.249f_{ck}^{0.772}$	ACI Committee 318(2014) $f_{t2}=0.56f_{ck}^{0.5}$	Anoglu et al (2006) $f_{t3}=0.387f_{ck}^{0.63}$	CEB-FIB (1991) $f_{t4}=0.3f_{ck}^{0.66}$	Gardner (1990) $f_{t5}=0.33f_{ck}^{0.667}$
44.89	4.38	4.70	3.75	4.25	3.70	4.17
53.87	5.26	5.41	4.11	4.77	4.17	4.71
62.85	6.13	6.09	4.44	5.26	4.61	5.22

The comparative results of table 2 show that the split tensile results measured is within the published results of other published authors.

**3.4 Results from Accelerated Corrosion Tests**

From equation 4 and 5

$$\Delta W = 25It \text{ (gms) for calculated mass loss.}$$

Where, I = corrosion current (amp) averages measured during accelerated corrosion (4.0, 2.4 and 2.0 milliamperes measured for concrete characteristic strength 35N/mm<sup>2</sup>, 30N/mm<sup>2</sup> and 25N/mm<sup>2</sup> respectively).

t = time (days).

$$\text{Corrosion Rate (mm/yr)} = 87.6 \times [w / (D \times A \times T)]$$

where W is the weight loss in milligrams measured as an average from corroded samples.

D is the density of the rebar used, g/cc, =7.8

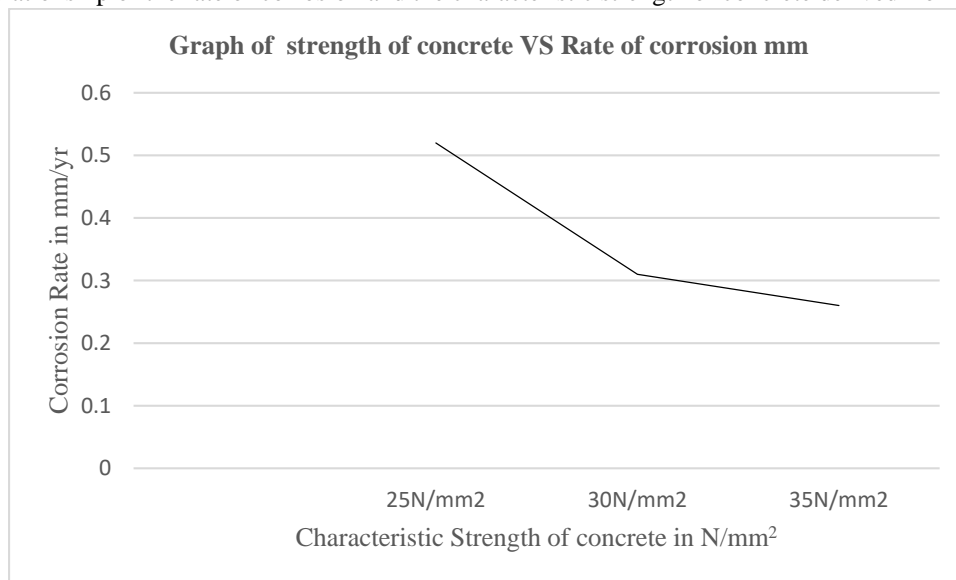
A is the surface area of the specimen subjected to corrosion (cm<sup>2</sup>), and =91.11

T is the duration of the test period in hours.

**Table 5: The rate of corrosion of rebar from samples from different diameter samples and strengths**

Concrete characteristic strength	Sample series	Rate of corrosion in mm/yr						
		Average mass of steel sample before corrosion (gms)	Average mass of steel sample after corrosion (gms)	Loss in weight (gms)measured	Loss in weight (gms) Calculated	Duration in days	Rate of corrosion mm/yr (measured)	Rate of corrosion mm/yr (calculated)
25N/mm <sup>2</sup>	150mm diameter	371	360.4	10.6	10.7	107	0.51	0.51
	130mm diameter	371	362.3	8.7	8.7	86	0.52	0.52
	100mm diameter	371	363.2	7.8	7.6	76	0.53	0.52
30N/mm <sup>2</sup>	150mm diameter	371	361.5	9.5	9.4	156	0.31	0.31
	130mm diameter	371	362.4	8.6	8.5	142	0.31	0.31
	100mm diameter	371	363.4	7.6	7.6	127	0.31	0.31
35N/mm <sup>2</sup>	150mm diameter	371	361.6	9.4	9.3	186	0.26	0.26
	130mm diameter	371	362.4	8.6	8.6	172	0.26	0.26
	100mm diameter	371	363.1	7.9	7.9	158	0.26	0.26

Graph 3 shows the Relationship of the rate of corrosion and the characteristic strength of concrete derived from table 5.



**Graph 3: Relationship of the rate of corrosion vs the rate of corrosion**

From table 5 and graph 3, it can be observed that the rate of corrosion is affected by the characteristic strength and this is attributed to the rate at which the aggressive chloride ions took to reach the rebar to enhance the onset of corrosion. It took a longest period for samples of characteristic 35N/mm<sup>2</sup> to corrode and result to a crack width of 0.2mm while samples with characteristic strength 25 N/mm<sup>2</sup> exhibited the shortest time. It can also be observed that concrete cover affects the duration of corrosion within the same characteristic strength of concrete but the rate of corrosion remains the same and this is because concrete of the same characteristic strength has the same electrical resistance.

### 3.4.1 Crack Initiation ( $t_1$ )

This is the first visible crack, which was observed through a magnifying glass ( $\times 1000$ ) and this period of time ( $t_1$ ) can be referred to as time to crack initiation.  $t_1$  depends on concrete tensile strength ( $f_t$ ). The model developed by Liu & Weyers (1996) reasonably predicts the time to first cracking although the predicted times are under-estimated (approximately 11%) when compared to results obtained from accelerated corrosion testing.

The time to crack initiation by Liu & Weyers (1996) model is the time when stresses resulting from the expansion of corrosion products exceed the tensile strength of concrete. The critical amount of corrosion products needed to cause first cracking consists of two parts:

- (i) the amount of corrosion products required to fill the total porous zone around the steel/concrete interface; and
- (ii) the amount of corrosion products then needed to generate the critical tensile stresses.

The time to cracking is influenced by corrosion rate, cover, bar spacing, concrete quality, and material properties. Therefore, the model proposed by Liu & Weyers (1996) was assumed herein as suitable for estimating the time to first cracking.

### 3.4.2 Crack Propagation ( $t_2$ )

Cracks first observed at the concrete surface through the magnifying glass were very small (width of less than 0.2mm) with lengths varying from 30mm to 300mm. Cracks width and length then increased in an inhomogeneous manner until they extended and joined together to create continuous corrosion-induced longitudinal cracking when the crack width was 0.2mm when the experiment stopped.

## 4.0 DETERIORATION MODEL

### i) Model development

Consider the schematic drawing shown in figure 5 for this research.

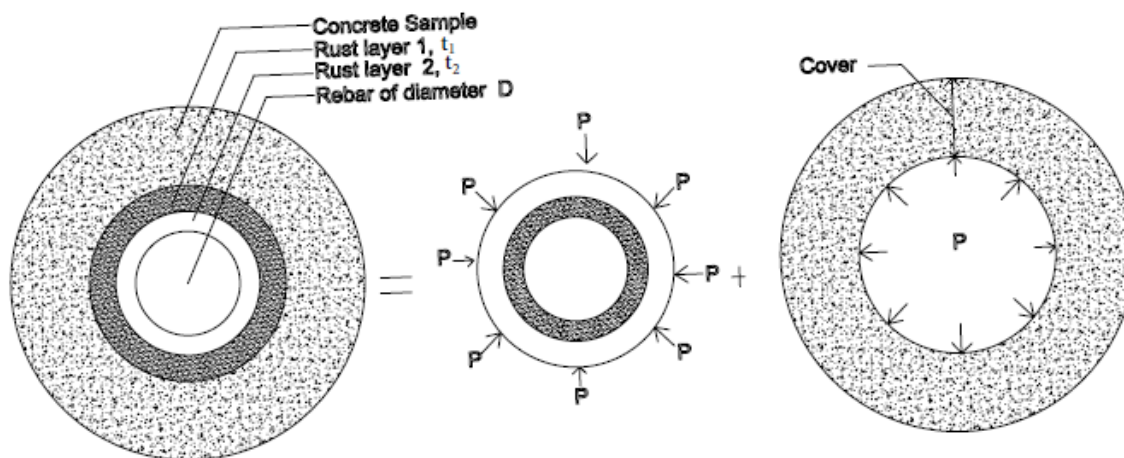


**Figure 5 Schematic drawing of expansive pressure on surrounding concrete due to accumulation of rust products**

Layer 2 is a transition zone between cement paste and aggregate and is influenced by the water/cement ratio, degree of consolidation and hydration, aggregate sizes and steel reinforcement. The weight of materials in this zone denoted as  $M_p$  can be expressed as,

$$M_p = \rho_{\text{rust}} V_p \tag{6}$$

where

$\rho_{\text{rust}}$  is the density of corrosion products and

$V_p$  is the total volume of interconnected pores around layer 2 of thickness  $t_1$ .

A steel bar having diameter  $D$  will increase its diameter to  $D+2t_1$ , when the mass of the amount of corrosion products reaches  $M_p$ . For a 300mm length of steel bar, since  $t_1 \ll D$ ,  $M_p$  can be estimated from equation 6,

$$M_p = 0.3\pi\rho_{\text{rust}} D t_1 \tag{7}$$

It can be seen that  $M_p$  is related to the size of the reinforcement, density of rust products and property of steel/concrete interface.

### ii) Estimation of $M_{\text{crit}}$

The critical amount of rust products to initiate a crack consists of two parts,  $M_p$ , the amount of corrosion products to fill the total interconnected pores around the steel/concrete interface (layer 2), and  $M_s$ , the amount of corrosion products that generate the critical tensile stresses, of 300mm length of steel bar, the value  $M_s$  can be estimated from equation 5,

$$\begin{aligned}
 M_s &= 0.3\pi\rho_{rust} [(t_1+t_2)(D+t_1+t_2)] \\
 &= 0.3\pi\rho_{rust} [D+(M_{st}/\rho_{st})] \\
 &= 0.3\rho_{rust} [\pi(t_1+t_2)D+(M_{st}/\rho_{st})]
 \end{aligned}
 \tag{8}$$

Where  $\rho_{rust}$ : the density of corrosion products

$\rho_{st}$ : the density of steel

$t_1$ : the thickness of the area around the steel/concrete interface and is the radial displacement under pressure

$t_2$ : the thickness of the corrosion products to generate the tensile stresses

$D$ : the diameter of the steel reinforcement

$M_{st}$ : mass loss of the rebar

Based on the theory of elasticity by Timoshenko and Goodier (1970) and Ugural (1986) and modelling the reinforced concrete as a thick wall cylinder under internal pressure  $P$ . The pressure  $P$  at concrete/rust products interface can be expressed as:

$$P = \frac{2E_{ef}t_2}{(D+2t_1)\left(\frac{b^2+a^2}{b^2-a^2}+v_c\right)}
 \tag{9}$$

where  $v_c$  is Poisson's ratio of the concrete,

$E_{ef}$  is an effective elastic modulus of the concrete

$a$  is the inner radius  $=(D+2t_1)/2$

$b$  is the outer radius  $=[C+(D+2t_1)/2]$ ,  $C$  is the cover in which

$E_{ef} = Ec/(1+jcr) = 1.16$

$Ec$  is elastic modulus of the concrete  $= 0.45\sqrt{fc} = 3.015$  and

$jcr$  is the creep coefficient of the concrete  $= 1.6$ .

$t_2$  is the thickness of the concrete under pressure

The thickness of concrete causing pressure is the thickness of corrosion products generating the pressure on the concrete.

At failure and considering that cracking first occurred over the reinforcement (the observed corrosion cracks were located along the thickness of the samples from the steel rebars to the edge of the sample and then longitudinally), the minimum stress required to cause cracking of the cover concrete equals the tensile strength of concrete,

$$P = \frac{2Cf_t}{D+2t_1}
 \tag{10}$$

where  $C$  is the cover depth of concrete

$f_t$  is the tensile strength of concrete.

From equations 6 and 7,  $t_2$  may be expressed as,

$$t_2 = \frac{cf_t}{E_{ef}} \left( \frac{a^2+b^2}{b^2-a^2} + v_c \right)
 \tag{11}$$

Therefore, the critical amount of corrosion products needed to induce cracking of the cover concrete can be estimated from equations 5 and 8,

$$M_{crit} = \rho_{rust} \left( 0.3\pi \left[ \frac{cf_t}{E_{ef}} \left( \frac{a^2+b^2}{b^2-a^2} + v_c \right) + t_1 \right] D + \frac{M_{st}}{\rho_{st}} \right)
 \tag{12}$$

From equation 9, the critical amount of corrosion products needed to induce cracking of the cover concrete is dependent on the tensile strength of concrete, cover depth, elastic modulus of concrete and properties of steel/concrete interface.

### iii) Growth of Rust Products

As the rust layer grows thicker, the ionic diffusion distance increases, and the rate of rust production decreases because the diffusion is inversely proportional to the oxide thickness. The rate of rust production can be written as follows,

$$\frac{dM_{rust}}{dt} = \frac{k_p}{M_{rust}}
 \tag{13}$$

where  $M_{rust}$  is amount of rust products (kg),

$t$  is corrosion time (years) and

$k_p$  is the rate of rust production and is related to the rate of rebar loss, which may be expressed in terms of corrosion rate,

$$k_p = 2.59 \times 10^{-6} \left( \frac{1}{\alpha} \right) \pi D i_{cor}
 \tag{14}$$

where  $\alpha$  is the ratio of the molecular weight of rust to that of iron,

$D$  is the steel diameter (cm.) and

$i_{cor}$  is the annual mean corrosion rate ( $\mu A/cm^2$ ).

Integrating equation 10, the growth of rust products can be obtained,

$$M_{rust}^2 = 2 \int_0^t 2.59 \times 10^{-6} (1/\alpha) \pi D i_{cor} dt \tag{15}$$

After calculating the corrosion rate from experimental data, the amount of rust products for a certain period of corrosion can be estimated.

**iv) Time to Cracking**

When the amount of corrosion products reaches the critical amount of rust products, the internal expansion stress will exceed the tensile strength of concrete and cause the cracking of the cover concrete. According to equation 11, for a constant corrosion rate, the time to cracking,  $t_{cr}$  can be given as follows:

$$t_{cr} = M_{crit}^2 / 2 [2.59 \times 10^{-6} (1/\alpha) \pi D i_{cor}] \tag{16}$$

where  $M_{crit}$  is the critical amount of corrosion products in kilograms. Since corrosion rate is a function of corrosion time as presented in equation 11, using the numerical method, the time to cracking can be also calculated from equation 16.

Table 6 Based on calculated critical amount of rust products is obtained from equation 12 and the times to cracking is obtained from equation 16. The results are summarized in Table 6. As it can be seen from the table in column 5 and 6, the measured times to cracking are within the predicted values by the model.

**Table 6: Parametric study of predicted and observed times to cracking of the research and the model**

Concrete characteristic strength	Sample series	Rebar diameter(mm)	Cover depth(mm)	Measured corrosion rate mm/year	Time in years Model predicted*	Time in years Measured
25N/mm <sup>2</sup>	100mm diameter x 300mm high	10	140	0.51	0.153-0.319	0.215
	130mm diameter x 300mm high	10	120	0.52	0.186-0.389	0.243
	150mm diameter x 300mm high	10	90	0.53	0.272-0.566	0.302
30N/mm <sup>2</sup>	100mm diameter x 300mm high	10	140	0.31	0.239-0.498	0.441
	130mm diameter x 300mm high	10	120	0.31	0.306-0.638	0.401
	150mm diameter x 300mm high	10	90	0.31	0.374-0.778	0.359
35N/mm <sup>2</sup>	100mm diameter x 300mm high	10	140	0.26	0.285-0.594	0.525
	130mm diameter x 300mm high	10	120	0.26	0.365-0.761	0.486
	150mm diameter x 300mm high	10	90	0.26	0.436-0.908	0.430

\*The model predicted times to cracking were calculated taking  $\alpha_1$  value of 1.8 for (FeO) and 3.75 for (Fe(OH)<sub>2</sub>) for corrosion products. [33]

From Table 6, it can be observed that the measured times to cracking are within the model predicted time.

## 5.0 Conclusions

The following conclusions can be made from this research:

1. The model proposed shows that amount of corrosion products to fill the total interconnected pores around the rebar/concrete interface (Mp) and the amount of corrosion products to generate the critical tensile stress (Ms) constitute the critical mass of corrosion products (M<sub>crit</sub>) to induce cracking of the concrete cover. The critical mass of corrosion products is influenced by the type of corrosion products, the cover to the rebar, the rebar size and the compressive strength of concrete and steel/concrete interface.
2. The time to corrosion model developed here, that is for a maximum crack width of 0.2mm as a specified limit of water structures shows that the time to corrosion cracking of the cover concrete in a chloride contaminated concrete structure is a function of reinforcement cover, concrete compressive strength, corrosion rate and critical mass of the corrosion products. The times to cracking predicted by the model are in good agreement with the observed times to cracking based on this research

## REFERENCES

- [1] United Nations (2015). "Transforming our world: the 2030 Agenda for Sustainable Development," Available from [www.un.org/ga/search/view\\_doc.asp?symbol=A/RES/70/1&Lang=E](http://www.un.org/ga/search/view_doc.asp?symbol=A/RES/70/1&Lang=E).
- [2] Hossein M. S., Keivan K., Alireza Hashemian A., (2010). *A model for the evolution of concrete deterioration due to reinforcement corrosion*. Mathematical and Computer Modelling 52: 1403-1422
- [3] Palanisamy G., (2019). "Corrosion Inhibitors," IntechOpen, DOI: 10.5772/intechopen.80542.
- [4] Mogire P.O., Abwodha S., Mweru J.N., Mangurui G.N., (2018), "The effect of Selected Cement Brands in Kenya on the Critical Penetration Depth of Rust in Reinforced Concrete Water Conveyancing Structures," International Journal of Scientific and Research Publications, 11: 2250-3153.
- [5] Ghods P., Isgor O.B., Bensebaa F., Kingston D., (2012). "Angle-resolved XPS study of carbon steel passivity and chloride-induced depassivation in simulated concrete pore solution," Corros. Sci. 58:159-167.
- [6] ACI Committee 222, "Protection of Metals in Concrete Against Corrosion," ACI 222R-01, American Concrete Institute, Farmington Hills, Michigan, 2001.
- [7] Alonso C, Andrade C, Rodriguez J, Diez J.M., (1998), "Factors controlling cracking of concrete affected by reinforcement corrosion," Mater and Struct 31: 435-441.
- [8] Bazant Z.P., (1979), "Physical model for steel corrosion in concrete sea structures – Application," J Struct Div 105(6): 1155-1166.
- [9] Liu Y, Weyers RE (1998), "Modeling the time-to-corrosion cracking in chloride contaminated reinforced concrete structures," ACI Mater J 95(6): 675-681.
- [10] Li C.Q., Melchers R.E, Zheng J.J., (2006), "Analytical model for corrosion-induced crack width in reinforced concrete structures," ACI Struct J 103(4): 479-487.
- [11] Molina F. J, Alonso C, Andrade C., (1993), "Cover cracking as a function of rebar corrosion: Part 2 – Numerical model," Mater and Struct 26: 532-548.
- [12] Du Y.G., Chan A.H.C., Clark L.A., (2006), "Finite element analysis of the effects of radial expansion of corroded reinforcement," Comp and Struct 84: 917-929.
- [13] Andrade, C., Alonso, C. and Molina, F. J. "Cover cracking as a function of bar corrosion: Part I—Experimental test," Mater. Struct. 26 (1993) 453-464.
- [14] Morinaga S. (1989). "Prediction of Service Lives of Reinforced Concrete Buildings based on Rate of Corrosion of Reinforcing Steel," Special report of the Institute of Technology, Japan, Skimiza Corporation.
- [15] Liu Y., Weyers R.E., (1998). "Modelling the time to corrosion in cracking in chloride contaminated reinforced concrete structures," ACI Mat. J. 95: 675-681.
- [16] Bhargava K., Ghosh A.K., Mori Y., Ramanujam S. (2006). "Model for cover cracking due to rebar corrosion in RC structures," Eng. Struct., 28: 1093-1109
- [17] Kiani K. (2002). "Study of reinforcement corrosion in RC structures via reproducing kernel particle method," M.Sc. Thesis. Tehran, Sharif University of Technology.
- [18] Andrade C. Alonso C., Molina F.J. (1993). "Cover cracking as a function of rebar corrosion: part 1-experimental test," Mater. Struct., 26: 453-464.
- [19] Lundgren K. (2002). "Modeling the effect of corrosion on bond in reinforced concrete," Mag. Concr. Res., 54: 165-173.
- [20] Bhargava K., Ghosh A.K., Mori Y., Ramanujam S. (2006). "Analytical model for time to cover cracking in RC structures due to rebar corrosion," Nucl. Eng. Des., 236: 1123-1139.
- [22] Bhargava K., Ghosh A.K., Mori Y., Ramanujam S. (2005). "Modeling of time to corrosion-induced cover cracking in reinforced concrete structures," Cem. Concr. Res., 35: 2203-2218.
- [23] P Mehta P.K., Monteiro P.J.M. (1997). "Concrete Microstructure, Properties and Materials," Indian Concrete Institute, Chennai, India.
- [24] Liu Y., (1996). "Modeling the time to corrosion cracking of the cover concrete in chloride contaminated reinforced concrete structures," Ph.D. Thesis, Blacksburg, Virginia Polytechnic Institute and State University, 1996.
- [25] Muhammad H.R., Khatun S., Uddin S.K.M., Nayeem M.A. (2010). "Effect of Strength and Covering on Concrete Corrosion," European Journal of Scientific Research, 4 (2010) 492-499
- [26] Visalakshi T. (2014). "Corrosion assessment in rebars of reinforced concrete structures using equivalent parameters extracted from piezo-patches," A PhD thesis in Civil engineering in India Institute of Technology, Delhi.
- [27] Kenya Bureau of Standards, KS EAS 18-1:2001-Cement Part 1: Composition, Specification and Conformity Criteria for Common Cements. Kenya Bureau of Standards, Nairobi, 2005.
- [28] Kumbhar, P.D. and Murnal, P.B. (2012), "Assessment of Suitability of Existing Mix Design Methods of Normal Concrete for Designing High Performance Concrete," International Journal of Civil and Structural Engineering, 3: 158-167.
- [39] Neville M. (1996). "Properties of Concrete," Pitman Publishing Company, London, UK.
- [30] Neville A.M., Brooks J.J. (2012). "Concrete Technology," Longman, London, UK.
- [31] BS 12, "Specification for Portland cement," BSI Publications, London, 1996.
- [32] Aperador W., Vera R., Carvajal A.M., (2012). "Evaluation of the cathodic protection applied to steel embedded in the ASS using the finite element method" International Journal of Electrochemical Science, 7(2012)12870. 5
- [33] Bhargava, K., Ghosh, A. K., Mori, Y., Ramanujam, S. (2005). "Modeling of time to corrosion-induced cover cracking in reinforced concrete structures." Cement and Concrete Research, 35: 2203-2218.

AUTHORS

**First Author** – Mogire Philip, PhD Student, Department of Civil and Construction Engineering, University of Nairobi, Kenya, philosiemo@yahoo.com

**Second Author** – Dr. John Mwero, Senior Lecturer, Department of Civil and Construction Engineering, University of Nairobi, Kenya, johnmwero1@gmail.com.

**Third Author** – Prof. Silvester Abuodha, Associate Professor, Department of Civil and Construction Engineering, University of Nairobi, Kenya, sochieng@yahoo.com

**Fourth Author** – Prof. Geoffrey Mang'uriu, Professor, Department of Civil, Construction and Environmental Engineering, Jomo Kenyatta University of Agriculture & Technology, gmanguriu@yahoo.co.uk

**Correspondence Author** – Mogire Philip , philosiemo@yahoo.com, +254 734 967 989